CHAPTER VI
PREPARATION OF DUAL-LEACHED POLYCAPROLACTONE-POLY(HYDROXYBUTYRATE) OR POLY(3-HYDROXYBUTYRATE-CO-3-HYDROXYVALERATE)/HYDROXYAPATITE POROUS SCAFFOLDS FOR BONE TISSUE ENGINEERING

6.1 Abstract

The goal of this study was to investigate the potential of polycaprolactone (PCL)-poly(hydroxybutyrate)(PHB)/hydroxyaptite(HA) and polycaprolactone(PCL)-poly(3-hydroxybutyrate-co-3-hydroxyvalerate)(PHBV)/hydroxyaptite(HA) composite scaffolds for using as the bone scaffolding materials. Well defined and interconnected pores were detected by scanning electron microscope (SEM) analysis. The blending of the PHB or PHBV and addition of HA in PCL scaffolds resulted in increase porosities of the scaffold and, the water absorption capacities of the scaffolds also increased. The HA addition in the PCL, PCL-PHB, and PCL-PHBV scaffolds and the blending of PHB or PHBV in PCL scaffolds resulted in an increase in compressive properties. An indirect cytotoxicity evaluation of all PCL-PHB/HA and PCL-PHBV/HA dual-leached scaffolds with mouse fibroblastic cells (L929) and mouse calvaria-derived pre-osteoblastic cell (MC3T3-E1) indicated all dual-leached scaffolds were posed as nontoxic to cells. The ability to support mouse calvaria-derived pre-osteoblastic cell (MC3T3-E1) attachment, proliferation, differentiation, and mineralization were also evaluated. During the attachment period (4, 8, 16 hours), the viability of MC3T3-E1 cells on PCL-PHB/HA and PCL-PHBV/HA dual-leached scaffolds were higher than that on tissue-culture polystyrene plate (TCPS) and the PCL/HA at any given time point and during the proliferation period (day 1-3), all PCL-PHB/HA and PCL-PHBV/HA dual-leached scaffolds were able to support the proliferation of MC3T3-E1 at higher levels to that cells on TCPS and PCL/HA. For mineralization, cells cultured on surfaces of PCL-20%PHB/HA dual-leached scaffold showed the highest mineral deposition.

(Key-words: Scaffold, PCL, Solvent casting/Particulate leaching method, PHB, PHBV, Hydroxyapatite)

6.2 Introduction

Tissue engineering facilitates the creation of biological substitutes to repair or replace the failing organs or tissues. One of the most promising approaches toward this direction is to grow cells on scaffolds that act as temporary support for cells during the regeneration of the target tissues, without losing the three dimensional (3D) stable structure.[1]

Consequently, tissue engineering typically involves the use of porous, bioresorbable scaffolds to serve as temporary, three-dimensional scaffolds to guide cell attachment, differentiation, proliferation, and subsequent tissue regeneration.[2] Recent research strongly suggests that the choice of scaffold material and its internal porous architecture significantly affect regenerate tissue type, structure, and function. In addition to possessing the appropriate material composition and internal pore architecture for regenerating a specific target tissue, scaffolds must also have mechanical properties appropriate to support the newly formed tissue.[3] Briefly, a biomaterial scaffold suitable for use in tissue engineering should be biodegradable and have nontoxic degradation products, be highly porous with an interconnected pore structure, have suitable physical and mechanical properties, and be biocompatible and suitable for cell attachment, proliferation, and differentiation.[4]

Conventional methods for scaffold fabrication rely on a variety of techniques involving the use of woven and non-woven fabrics, solvent casting and particulate leaching, solution casting and gel casting with porogens, pressurized gas foaming, forging, injection molding, cold or hot pressing, and electrospinning.[5] The solvent casting/salt leaching method has the advantage of controlling pore size by manipulating the size of the salt particulate. Techniques like freeze-drying often allow the fabrication of porous scaffolds with a high compressive modulus. Researchers have used combinations of these techniques to obtain desirable porosity ratios and pore dimensions.[6]

Polycaprolactone (PCL), poly(lactic acid) (PLA), poly(glycolic acid) (PGA), poly(hydroxy butyrate) (PHB), and poly(3-hydroxybutyrate-co-3-hydroxyvalerate) (PHBV) and poly(butylene succinate) (PBS) are examples of synthetic biodegradable polymers. PCL, PHB and PHBV are extensively used in

tissue engineering for treating patients suffering from damaged or lost organs or tissues. [7-10] They have been demonstrated to be biocompatible, degrading into non-toxic components, and have a long history with FDA (US Food and Drug Administration) approval for clinical use. [11-14] In general, scaffolds must exhibit high porosity, proper pore size, biocompatibility, biodegradability and proper degradation rate. The scaffold must provide sufficient mechanical support to maintain stresses and loadings generated during in vitro or in vivo regeneration. [1]

PCL is also an important member of the aliphatic polyester family. [15] PCL degrades at a significantly slower rate than PLA, PGA, and PLGA. The slow degradation makes PCL less attractive for biomedical applications, but more attractive for long-term implants and controlled release application. [16] PCL has been used as a candidate polymer for bone tissue engineering, where scaffolds should maintain physical and mechanical properties for at least 6 months. [1] Polyhydroxyalkanoates (PHA) have been demonstrated to be a family of biopolymers with good biodegradability and noncytotoxicity. [17] Poly(3-hydroxybutyrate) (PHB) and and poly(3-hydroxybutyrate-co-3-hydroxyvalerate) (PHBV), as the member of polyhydroxyalkanoates (PHA) family, have attracted much attention for a variety of medical applications because of its biodegradation and excellent biocompatibility. [18] Polymers like poly(3-hydroxybutyrate) (PHB), poly(hydroxybutyrate-co-hydroxyvalerate) (PHBV) and poly(lactic acid) (PLA) have attracted much attention recently because of their excellent biodegradability and biocompatibility. However, the brittleness and narrow processing window of these polymers restrict their application. Blending of these polymers with other biocompatible polymers has been widely studied to improve their mechanical and thermal properties [18]

Other important categories of materials are bioactive ceramics such as calcium phosphates (with hydroxyapatite being the prominent family member), bioactive glasses, and glassceramics which elicit a specific biological response at the interface of the material resulting in the formation of a strong bond between the bone tissue and the material. [19-22] Currently, polymer/ceramic composite materials are being developed with the aim of enhancing mechanical properties and improving cell and tissue interaction of scaffolds . Nanocomposites based on HA particles and

biopolymers have attracted attention for their good osteoconductivity, osteoinductivity, biodegradability and high mechanical strengths PCL/nHA nanocomposites were prepared and they combine the osteoconductivity and biocompatibility shown by HA ceramic with PCL properties.[19,23-27]

In recent years, many studies have been carried out on composite scaffolds consisting of PHB or PHBV reinforced with bioactive ceramics. Incorporation of HA microparticles into PHB or PHBV resulted in composites with improved mechanical properties and in vitro bioactivity. [19] While the blended polymers play an important role in the development of microporous controlled-delivery systems. The PCL-PHB and PCL-PHBV dual-leached scaffolds in our previous work provided better support for bone cell adhesion and proliferation.[28] Therefore, the objective of this work were to prepare the PCL-PHB/HA and PCL-PHBV/HA dual leached scaffolds, and improve the mechanical properties of the dual-leached PCL-PHB and PCL-PHBV scaffolds by the addition of hydroxyapatite. The water absorption capacities, degradation behavior, morphology, physical and mechanical properties of the PCL-PHB/HA and PCL-PHBV/HA dual-leached scaffolds were investigated. Then, the indiect cytotoxicity of L929 and MC3T3-E1, MC3T3-E1 cell attachment, proliferation, and differentiation were also evaluated the potential of scaffolds for used in bone-tissue engineering applications.

6.3 Experimental

6.3.1 Materials

Polycaprolactone (PCL; MW = 80,000 $gmol^{-1}$), poly(3-hydroxybutyrate) (PHB; MW= 300,000 $gmol^{-1}$), poly(3-hydroxybutyrate-co-3-hydroxyvalerate) (PHBV; MW = 680,000 $gmol^{-1}$) and calcium hydroxide ($Ca(OH)_2$) were purchased from Sigma-Aldrich, USA. Phosphoric acid (H_3PO_4) and chloroform were purchased from Labscan (Asia), Thailand. Polyethylene glycol (PEG; MW = 1,000 $gmol^{-1}$; Merck, Germany) and sodium chloride (Ajax Finechem,

Australia) were used as porogen. All other chemicals were of analytical reagent grade and used without further purification.

6.3.2 Preparation of PCL-PHB/HA and PCL-PHBV/HA Scaffolds

Blends of 10%, 20% and 30% w/w PHB-PCL/HA and 10%, 20% and 30% w/w PHBV-PCL/HA dual-leached scaffolds were fabricated by the solvent casting, polymer leaching and salt particulate leaching technique. An equal mass of polymer and PEG was first dissolved in chloroform at the concentration of 28% w/v to obtain a blend solution of the polymers, then the amount of HA powder (50%w/w of polymer) which was synthesized according to the procedure proposed by Lee et al[33] were added to the solution. NaCl particles, a *priori* sieved to obtain particles with diameters in the range of 400-500 μm, were then added into PCL-PHB/HA and PCL-PHBV/HA solutions at the polymer to NaCl ratio = 1:30% w/w. The mixture was then packed into Petri dishes and the cylindrical mold with the dimension of 1.2 mm in diameter and 0.8 mm in thickness. The molds were then placed in the hood overnight for solvent evaporation. After the time, the materials were immersed in deionized(DI) water for 48 hr with repeated change of DI water every 8 hr for leaching out the PEG and salt particles. Scaffolds were air-dried for 24 h and vacuum-dried overnight. For sterilization, the scaffolds were placed in 70% v/v ethanol for 30 min and washed with sterilized deionized water.

6.3.3 Characterization

Microstructure Observation

The pore morphology, size, distribution, and interconnectivity of the porous scaffolds were observed using a JEOL JSM-5200 scanning electron microscope. One cylindrical scaffold was randomly selected from each group, cut with a razor blade in the middle and mounted onto a stub. These cross sections were coated with a thin film of gold using a JEOL JFC-1100E sputtering device for 5 min prior to observation by scanning electron microscopy (SEM).

Porosity, Pore Volume, and Pore Size

The porosity and pore volume of the scaffolds were determined gravimetrically, according to the following equations:

$$\text{Porosity}(\%) = \left(1 - \frac{\rho \text{scaffold}}{\rho \text{polymer}}\right) x \ 100$$

$$\text{Pore volume} = \left(\frac{1}{\rho\text{scaffold}} - \frac{1}{\rho\text{polymer}}\right) x\ 100$$

where $\rho_{polymer}$ is the density of the polymer from which the scaffolds were fabricated, and $\rho_{scaffold}$ is the apparent density of the scaffolds, determined using a Sartorius YDK01 density measurement kit. Here, ρ_{PCL} was considered to be 1.145 gcm^{-1}. Five specimens were assessed for both porosity and pore volume, and an average value was calculated for each property. In contrast, the pore size of each scaffold was directly measured from the SEM images using a SemAfore Digital slow-scan image-recording system (version 5.0 software). At least 30 pores for each of the cross and longitudinal sections (i.e., at least 60 pores in total) were analyzed, and average values were calculated for all of the scaffolds investigated.

Water Absorption Capacity

The scaffold specimens were cut from the molds, which were created by casting in Petri dishes with a circular shape measuring 15 mm in diameter and 3 mm in height. The constructs were first dried, weighed, and individually immersed in 10 mL of 10 mM phosphate-buffered saline (PBS; pH 7.4) at room temperature. At a specified point in time, the specimens were removed from the solution, carefully placed on glass for 5 sec to remove any excess water, and weighed immediately. The amount of water retained in each scaffold was determined according to the following equation:

$$\text{Water absorption}(\%) = \frac{(Ww - Wd)}{Ww} x\ 100$$

where W_d and W_w are the weights of the specimen before and after submersion in the medium, respectively. This experiment was conducted in pentuplicate, and measurements were performed at different time points within a period of 7 d.

Compressive Modulus

The compressive modulus of each scaffold was determined using a universal testing machine (Lloyd LRX, UK) and a load cell of 500 N in a dry state at room temperature. The load was vertically compressed at a crosshead speed of 3 mm/min until the scaffolds were reduced to approximately 70% of the original thickness. The initial compressive modulus was then determined from the slope of

the linear portion of the stress-strain curve at a compressive strain of 20%.

Degradation

The degradation of all scaffolds had been examined up to 13 weeks. Briefly, 5 scaffolds from each type of material had been separately immersed in 5 ml of 0.1M PBS, pH 7.4 with or without lipase (*Pseudomonas sp.*, 45 units/l). The samples were kept at 37°C up to 13 weeks with the replacing of new medium at every 84 hr throughout the experiment in order to keep enzymatic activity at the constant level. The samples were taken out at every 2 weeks, washed thoroughly with distilled water and dried at room temperature for 24 hr and in a vacuum for another 48 hr. The remaining weight of the scaffolds was investigated. The scaffold remaining weight was measured and calculated by the following equation.

$$\text{Remaining weight}(\%) = \frac{W_t}{W_0} \ x \ 100$$

where W_0 is the initial weight and W_t is the weight of the scaffold at a single degradation time point. An average remaining weight was calculated from those of five samples in each group.

6.3.4 Biological Evaluation

Cell Culturing

Mouse fibroblasts (L929) and mouse calvaria-derived pre-osteoblastic cells (MC3T3-E1) were used as reference cell lines. The L929 cells were cultured as a monolayer in Dulbecco's modified Eagle's medium (DMEM; Sigma-Aldrich, USA) supplemented with 10% fetal bovine serum (FBS; BIOCHROM AG); 1% L-glutamine (Invitrogen); and 1% antibiotic and antimycotic formulation, containing penicillin G sodium, streptomycin sulfate, and amphotericin B (Invitrogen, USA). The MC3T3-E1 cells were cultured in Minimum Essential Medium (MEM; Hyclone, USA) with Earle's Balanced Salts and supplemented with 10% FBS (BIOCHROM AG, Germany), 1% L-glutamine (Invitrogen, USA), and 1% antibiotic and antimycotic formulation, as described above. The media were replaced every 2 days, and the cultures were maintained at 37°C in a humidified atmosphere containing 5% CO_2.

Each scaffold was cut into circular discs of approximately 15 mm in diameter, which were placed into the wells of a 24-well tissue-culture polystyrene

(TCPS) plate. The discs were then sterilized in 70% ethanol for 30 min, washed with autoclaved DI water and PBS, and immersed in MEM overnight. To ensure complete contact between the scaffolds and the wells, each construct was pressed with a metal ring of approximately 12 mm in diameter.

The cultured MC3T3-E1 cells were detached using 0.25% trypsin containing 1 mM EDTA (Invitrogen, USA) and counted with a hemacytometer (Hausser Scientific, USA). The cells were then seeded on the scaffolds at a density of approximately 40,000 cells/well for the attachment and proliferation studies. Seeded, empty wells of a TCPS plate were used as a control. For the indirect cytotoxicity, alkaline phosphatase activity, and mineralization evaluations, the MC3T3-E1 cells were seeded at a density of approximately 40,000 cells/well on the scaffolds and empty wells of a TCPS plate. The culture was maintained in an incubator at 37°C with a humidified atmosphere containing 5% CO_2.

Indirect Cytotoxicity Evaluation

Two cell types were used for the cytotoxicity evaluation: 1) mouse calvaria-derived pre-osteoblastic cells (MC3T3-E1) and 2) mouse fibroblasts (L929). In particular, an indirect cytotoxicity test was conducted on TCPS wells and on PCL/HA, PCL-10%PHB /HA, PCL-20%PHB /HA, PCL-30%PHB/HA, PCL-10%PHBV/HA, PCL-20%PHBV/HA and PCL-30%PHBV/HA scaffolds. First, the extraction media were prepared by immersing the samples, which were approximately 15 mm in diameter, in serum-free medium (SFM) containing DMEM (for the L929 cells) or MEM (for the MC3T3-E1 cells), supplemented with 1% L-glutamine, 1% lactalbumin, and 1% antibiotic and antimycotic formulation, for 1, 3, or 7 days. Each of these extraction media was then used to evaluate the cytotoxicity of the scaffolds. Either the L929 cells or the MC3T3-E1 cells were cultured in the wells of a 24-well culture plate containing 10% FBS-supplemented DMEM or MEM, respectively, for 16 h to allow cell attachment to the plate. Next, the cells were starved in SFM for 24 h, after which the medium was replaced with extraction medium. After an additional 24 h of cell culture, a 3-(4,5-dimethylthiazol-2-yl)-2,5-diphenyl-tetrazolium bromide (MTT) assay was performed to quantify the number of viable cells. These experiments were conducted in triplicate.

MTT Assay

The MTT assay is based on the reduction of yellow tetrazolium salt to purple formazan crystals by dehydrogenases secreted by the mitochondria of metabolically active cells. The amount of purple formazan crystals formed is proportional to the number of viable cells. In the current study, the culture medium was first aspirated and replaced with 400 µL/well of MTT solution at 0.5 mg/mL in a 24-well culture plate. Second, each plate was incubated for 30 min at 37°C. The MTT solution was then aspirated, and 1 mL/well of dimethyl sulfoxide (DMSO) containing 125 µL/well of glycine buffer (pH 10) was added to dissolve the formazan crystals. Finally, after 5 min of rotary agitation, the absorbance of the DMSO solution at 540 nm was measured using a Thermo Spectronic Genesis10 UV/Visible spectrophotometer.

Cell Attachment and Proliferation

Cell behaviors, such as adhesion and proliferation, represent the initial phase of cell-scaffold communication, which subsequently affects cell differentiation and mineralization. In the attachment study, the MC3T3-E1 cells were allowed to adhere to the TCPS, PCL/HA, PCL-10%PHB /HA, PCL-20%PHB /HA, PCL-30%PHB/HA, PCL-10%PHBV/HA, PCL-20%PHBV/HA and PCL-30%PHBV/HA scaffolds for 4, 8 or 16 h. Each sample was then rinsed with PBS to remove unattached cells prior to morphological assessment of the adherent cells by SEM. In the proliferation study, the viability of the cells on the scaffolds was determined after 1, 2, or 3 days of cell culture by Alamar Blue Assay. These experiments were performed in triplicate.

Alamar Blue Assay

Resazurin, the active ingredient of alamarBlue reagent, is a non-toxic, cell permeable compound that is blue in color and virtually non-fluorescent. Upon entering cells, resazurin is reduced to resorufin, a compound that is red in color and highly fluorescent. Viable cells continuously convert resazurin to resorufin, increasing the overall fluorescence and color of the media surrounding cells. First, each culture medium was removed and replaced with 500 µL/well of 10% alamar blue solution for a 24-well culture plate. Secondly, the plate was incubated for 3 hours at 37 °C. Finally, the fluorescent emission intensity of the obtained solution

was then measured at 585 nm, after it had been excited at 570 nm, using the microplate reader.

Morphological Observation of Cultured Cells

After removal of the culture medium, the cell-seeded scaffolds were rinsed twice with PBS and fixed in 3% glutaraldehyde solution, which was diluted from 50% glutaraldehyde solution (Sigma, USA) with PBS, at 500 μL/well. After 30 min, the wells were again rinsed with PBS. Following cell fixation, the specimens were dehydrated in ethanol solutions of varying concentrations (i.e., 30, 50, 70, 90, and 100%) for approximately 2 min at each concentration and dried in 100% hexamethyldisilazane (HMDS; Sigma, USA) for 5 min. The scaffolds were allowed to air-dry after the removal of the HMDS. The completely dry specimens were mounted on SEM stubs, coated with gold, and observed using a JEOL JSM-5200 scanning electron microscope.

Production of Alkaline Phosphatase (ALP) by Cultured Cells

The ALP activity of the MC3T3-E1 cells was measured using Alkaline Phosphate Yellow Liquid. In this reaction, ALP catalyzes the hydrolysis of the colorless organic phosphate-ester substrate p-nitrophenyl phosphate (pNPP) to a yellow product, p-nitrophenol, and a phosphate. In the present study, the MC3T3-E1 cells were cultured on scaffold specimens for 3, 5, or 7 days to observe the production of ALP. The specimens were then rinsed twice with PBS after the removal of the culture medium. Alkaline lysis buffer (10 mM Tris-HCl, 2 mM $MgCl_2$, and 0.1% Triton X-100, pH 10 was added at 200 μL/well, and the samples were scraped and frozen at -20°C for at least 30 min prior to the next step. An aqueous solution of 2 mg/mL pNPP (Zymed Laboratories, USA) mixed with 0.1 M amino propanol (10 μL/well) in 2 mM $MgCl_2$ (100 μL/well) at a pH 10.5 was prepared and added to the specimens (110 μL/well), followed by incubation at 37°C for 15 min. The reaction was stopped by adding 900 μL/well of 50 mM NaOH, and the extracted solution was transferred to a cuvette and placed in the UV-visible spectrophotometer, from which the absorbance at 410 nm was measured. The amount of ALP was then calculated using a standard curve. To determine the ALP activity, the amount of ALP was normalized to the total amount of protein synthesized.

In the protein assay, the samples were treated in the same manner as in the ALP assay up to the point at which the specimens were frozen. After freezing, bicinchoninic acid (BCA; Pierce Biotechnology, USA) solution was added to the scaffolds, which were then incubated at 37°C for 15 min. The absorbance of the medium was measured at 562 nm using the UV-visible spectrophotometer, and the total amount of protein was calculated using a standard curve.

Mineralization Analysis

Alizarin Red S dye binds selectively to calcium salts and is widely used for mineral staining (i.e., the staining product is an Alizarin Red S calcium chelating product). The isolated MC3T3-E1 cells were plated on 24-well plates at 40,000 cells/well and maintained in culture medium. After 24 h, the cultures were treated with medium supplemented with 50 μg/ml ascorbic acid (Sigma, USA), 5 mM β-glycerophosphate (Sigma, USA), and 0.2 μg/mL dexamethasone (Sigma, USA), which was replaced every 2 days. After 14 and 21 days of treatment, the cells were washed with PBS, fixed in ice-cold absolute methanol for 10 min, and stained with 1% Alizarin Red S in DI water (Sigma, USA) at pH 4.2 for 2-3 min. After removing the alizarin red S solution, the cells were rinsed with DI water and dried at room temperature. The images of each culture were captured, and the stain was extracted using 10% cetylpyridinium chloride (Sigma, USA) in 10 mM sodium phosphate for 1 h. The absorbance of the collected dye was read at 570 nm using a UV-visible spectrophotometer (Thermo Spectronics Genesis10).

6.3.5 Statistical Analysis

All of the values were expressed as the mean ± standard deviation. Statistical analyses of the different data groups were performed by one-way analysis of variance (ANOVA), along with the least-significant difference (LSD) test, using SPSS software version 11.5. Values with $p < 0.05$ were considered statistically significant.

\

6.4 Results and Discussion

6.4.1 Characterization of PCL-PHB/HA and PCL-PHBV/HA Scaffolds

Microstructure Observation

Table 6.1 show the SEM micrographs of the PCL/HA, PCL-PHB/HA, and PCL-PHBV/HA microporous scaffolds. The porous structure and the interconnected networks were created by NaCl and PEG leaching in aqueous medium. From the SEM analysis of PCL/HA, PCL-PHB/HA, and PCL-PHBV/HA porous scaffolds, the well defined and interconnected pores were detedcted by the resulted from the use of both salt and PEG. The interconnected pores were formed in scaffolds after PEG was leached out. SEM images of PCL-PHB/HA and PCL-PHBV/HA dual-leached scaffolds showed that both scaffold types exhibited a similar porous structure to the PCL/HA dual-leached scaffold.

Table 6.2 show the pore size of PCL/HA, PCL-PHB/HA and PCL-PHBV/HA dual-leached scaffolds. The pore dimensions of the PCL/HA, PCL-10%PHB/HA, PCL-20%PHB/HA, PCL-30%PHB/HA, PCL-10%PHBV/HA, PCL-20%PHBV/HA, and PCL-30%PHBV/HA dual-leached scaffolds are in the range of 441 ± 23, 372 ± 23, 374 ± 30, 379 ± 21, 367 ± 28, 389 ± 24, and 379 ± 27 respectively. The size of pores in PCL/HA dual-leached scaffold was larger than PCL-PHB/HA and PCL-PHBV/HA dual-leached scaffolds. The size of pores in PCL-PHB/HA and PCL-PHBV/HA scaffolds were larger than the pores of the PCL-PHB and PCL-PHBV dual-leached scaffolds. SEM images revealed that the PCL-PHB/HA and PCL-PHBV/HA dual-leached scaffolds presented with decreased microporosity when compared to PCL dual-leached scaffold, indicating that blending of PHB and PHBV and addition of HA affected the processing of the scaffold. Moreover they also showed the present of macropore interconnectivity and the presence of PHB and PHBV matrix and HA particles distributed within the PCL matrix.

Table 6.1 SEM images at 50x, and 200x magnification illustrating the microstructures of the PCL/HA, PCL-PHB/HA, and PCL-PHBV/HA dual-leached scaffolds
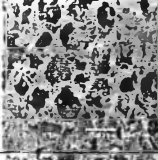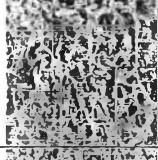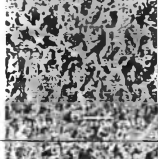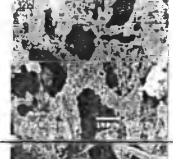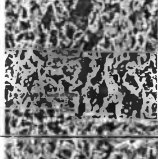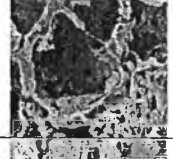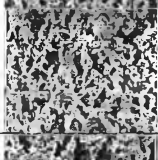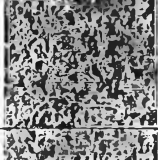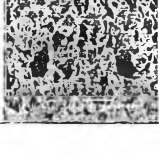
Scaffolds	Magnification	
	50x	200x
PCL/HA		
PCL-10% PHB/HA		
PCL-20% PHB/HA		
PCL-30% PHB/HA		
PCL-10% PHBV/HA		
PCL-20% PHBV/HA		
PCL-30% PHBV/HA		

Table 6.2   Actual HA, density, percentage of porosity, pore volume, and compressive modulus of the PCL/HA, PCL-PHB/HA and PCL-PHBV/HA dual-leached scaffolds: a,b,c,d, e , f are significantly different at p < 0.05 for an individual feature; *one way ANOVA with Tukey HSD, and n = 10 for porosity pore volume. n = 30 for pore size

Scaffolds	Actual HA (%)	Density* (g/cm³)	Porosity* (%)	Pore volume* (cm³/g)	Pore size (μm)	Compressive modulus (kPa)
PCL/HA	29.29	0.3276±0.0396	71.39±3.46	2.2202±0.3820	441±23	258±24.1
PCL-10% PHB/HA	26.36	0.2263±0.0669	80.23±5.85	3.9890±1.7719	372±23	1778±7.8
PCL-20% PHB/HA	31.46	0.2135±0.0446	81.36±3.89	4.0337±1.2328	374±30	1745±6.1
PCL-30% PHB/HA	26.20	0.2119±0.0359	81.50±3.13	3.9755±0.7257	379±21	1,923±9.5
PCL-10% PHBV/ HA	36.22	0.2614±0.0383	77.17±3.34	3.0355±0.6380	367±28	2,283±7.7
PCL-20% PHBV/ HA	36.96	0.2391±0.0319	79.11±2.72	3.3703±0.5336	389±34	1,712±17.6
PCL-30% PHBV/ HA	36.07	0.2077±0.0300	81.86±2.62	4.0344±0.7278	379±27	2,866±29.6

Density, Porosity, and Pore volume

The actual amount of HA, density, the porosity, and the pore volume of the PCL/HA, PCL-10%PHB /HA, PCL-20%PHB /HA, PCL-30%PHB/HA, PCL-10%PHBV/HA, PCL-20%PHBV/HA and PCL-30%PHBV/HA scaffolds that had been prepared as a function of the initial HA content 50% w/w are shown in table 6.2. From the TGA information of the char contents at 900 °C in the thermograms, they could be refered to the actual amounts of the HA particles within PCL/HA, PCL-10%PHB /HA, PCL-20%PHB /HA, PCL-30%PHB/HA, PCL-10%PHBV/HA, PCL-20%PHBV/HA and PCL-30%PHBV/HA dual-leached scaffolds. For the PCL/HA PCL-10%PHB /HA, PCL-20%PHB /HA, PCL-30%PHB/HA, PCL-10%PHBV/HA, PCL-20%PHBV/HA and PCL-30%PHBV/HA dual-leached scaffolds that had been prepared with the initial HA content of 50%w/w, the actual amounts of HA were determined to be 29.29, 26.36, 31.46, 26.20, 36.22, 36.96, and

36.07%w/w, respectively. For the PCL-PHB/HA scaffolds, the difference between the initial and actual content were higher than the PCL-PHBV/HA scaffolds.

The porosity of the PCL/HA scaffolds was 71.39% on average, whereas the porosity of the PCL-PHB/HA and PCL-PHBV/HA scaffolds ranged from 80.23-81.50% and 77.17-81.86% on average (n = 10). In particular, the porosity increased from approximately 71.39% for the PCL/HA scaffolds to approximately 80.23% for the PCL-10%PHB/HA scaffolds, 81.36% for the PCL-20%PHB/HA scaffolds, 81.50% for the PCL-30%PHB/HA scaffolds, 77.17% for the PCL-10%PHBV/HA scaffolds, 79.11% for the PCL-20%PHBV/HA scaffolds, and 81.86% for the PCL-30%PHBV/HA scaffolds.

The density of PCL/HA scaffold was 0.3276 g/cm^3 and the density of PCL-PHB/HA and PCL-PHBV/HA scaffolds were 0.2119-0.2263 g/cm^3 and 0.2077-0.2614 g/cm^3. Whereas the density value decreased with the blending of PHB or PHBV, that is, from about 0.3276 g/cm^3 on average for the PCL dual-leached scaffold to about 0.2263 g/cm^3 on average for the PCL-10%PHB scaffold, 0.2135 g/cm^3 on average for the PCL-20%PHB scaffold, 0.2119 g/cm^3 on average for the PCL-30%PHB scaffold, 0.2614 g/cm^3 on average for the PCL-10%PHBV scaffold, 0.2391 g/cm^3 on average for the PCL-20%PHBV scaffold, and 0.2077 g/cm^3 on average for the PCL-30%PHBV scaffold (n=10). Specially, pore volume increased from 2.2202 cm^{3}g^{-1} for PCL scaffold to 3.9890 cm^{3}g^{-1} PCL-10%PHB scaffold, 4.0337 cm^{3}g^{-1} PCL-20%PHB scaffold, 3.9755 cm^{3}g^{-1} PCL-30%PHB scaffold, 3.0355 cm^{3}g^{-1} PCL-10%PHBV scaffold, 3.3703 cm^{3}g^{-1} PCL-20%PHBV scaffold, and 4.0344 cm^{3}g^{-1} PCL-30%PHBV scaffold. The pore volume decreased with an decreased the porosity. The blending of PHB or PHBV and HA decreased the density but increased the porosity values of the scaffolds. The porosity values increase with blending of PHB or PHBV and HA because both of PHB or PHBV and HA might be effect to free space available in pores.

Table 6.2 Actual HA, density, percentage of porosity, pore volume, and compressive modulus of the PCL/HA, PCL-PHB/HA and PCL-PHBV/HA dual-leached scaffolds: a,b,c,d, e , f are significantly different at $p < 0.05$ for an individual feature; *one way ANOVA with Tukey HSD, and n = 10 for porosity pore volume. n = 30 for pore size

Scaffolds	Actual HA (%)	Density* (g/cm^3)	Porosity* (%)	Pore volume* (cm^3/g)	Pore size (μm)	Compressive modulus (kPa)
PCL/HA	29.29	0.3276±0.0396	71.39±3.46	2.2202±0.3820	441±23	258±24.1
PCL-10% PHB/HA	26.36	0.2263±0.0669	80.23±5.85	3.9890±1.7719	372±23	1778±7.8
PCL-20% PHB/HA	31.46	0.2135±0.0446	81.36±3.89	4.0337±1.2328	374±30	1745±6.1
PCL-30% PHB/HA	26.20	0.2119±0.0359	81.50±3.13	3.9755±0.7257	379±21	1,923±9.5
PCL-10% PHBV/ HA	36.22	0.2614±0.0383	77.17±3.34	3.0355±0.6380	367±28	2,283±7.7
PCL-20% PHBV/ HA	36.96	0.2391±0.0319	79.11±2.72	3.3703±0.5336	389±34	1,712±17.6
PCL-30% PHBV/ HA	36.07	0.2077±0.0300	81.86±2.62	4.0344±0.7278	379±27	2,866±29.6

Water Absorption Capacity

Figure 6.1 illustrates the water absorption capacities of the PCL/HA, PCL-PHB/HA and PCL-PHBV/HA scaffolds in 0.1 M PBS at room temperature within 3 days. The water absorption rate increased rapidly in the early 1 h and slightly increased in 3 d for PCL/HA, PCL-10%PHB/HA, and PCL-20%PHB/HA scaffolds. The water absorption rate of PCL-30%PHB/HA rapidly increased in 12 h, and slightly increased in 3 d while the water absorption rate of PCL-PHBV/HA increased rapidly in 12 h, and increased continuously in 3 d. The water absorption capacities of PCL-PHB/HA and PCL-PHBV/HA scaffolds were lower than the water absorption capacities of PCL/HA scaffold at the early time point and were higher than the water absorption capacities of PCL/HA scaffold in 3d. The water absorption capacities of PCL-PHB/HA scaffold were lower than the water absorption capacities of PCL-PHBV/HA scaffolds at the early time point and were similar to the water absorption capacities of PCL-PHBV/HA scaffold at 3d. The blending of the PHB or

PHBV in PCL/HA scaffolds resulted in increase porosities of the scaffold and, the water absorption capacities of the scaffolds also increased.
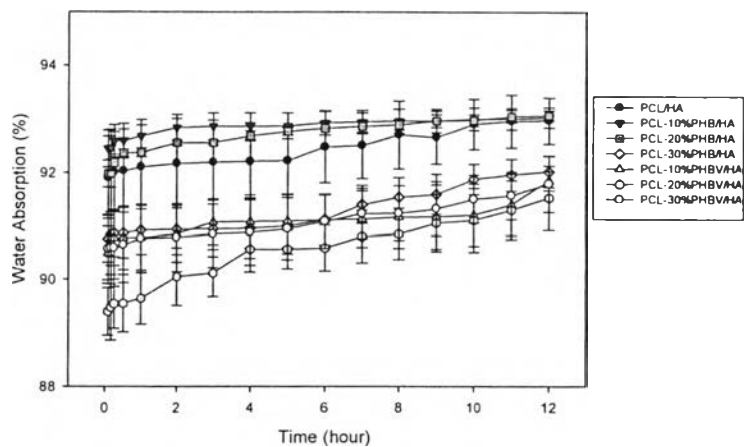
(a)
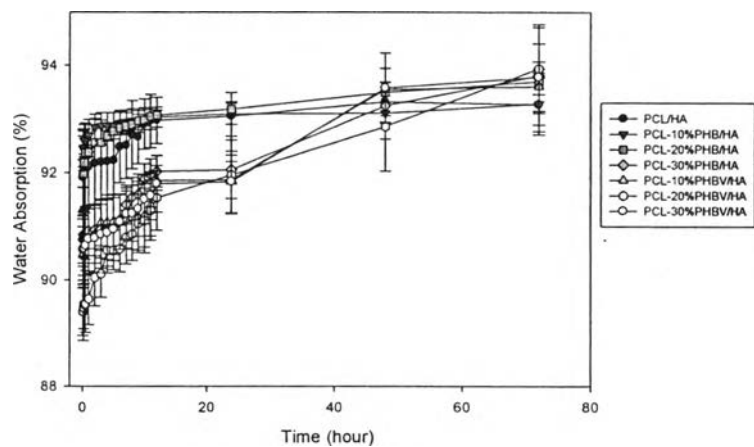
(b)

Figure 6.1 (a) Water absorption capacity of PCL/HA, PCL-PHB/HA, and PCL-PHBV/HA dual-leached scaffolds in 0.1 M PBS at room temperature over 12 hours. (b) Water absorption capacity of PCL/HA, PCL-PHB/HA, and PCL-PHBV/HA dual-leached scaffolds in 0.1 M PBS at room temperature over 3 days.

Compressive Modulus

The mechanical properties of porous scaffolds are evaluated by compressive tests. The compressive modulus of PCL/HA, PCL-PHB/HA and PCL-PHBV/HA scaffolds are shown in table 6.2. Compared with PCL/HA scaffold, PCL-PHB/HA and PCL-PHBV/HA scaffolds exhibit higher compressive modulus. The compressive modulus increased from ~ 258 kPa for the PCL/HA scaffold to 1778, 1745, 1923, 2283, 1712, and 2866 kPa for PCL-10%PHB/HA, PCL-20%PHB/HA, PCL-30%PHB/HA, PCL-10%PHBV/HA, PCL-20%PHBV/HA and PCL-30%PHBV/HA scaffolds, respectively. The HA addition in the PCL, PCL-PHB, and PCL-PHBV scaffolds and the blending of PHB or PHBV in PCL scaffolds resulted in an increase in compressive properties.

Table 6.2 Actual HA, density, percentage of porosity, pore volume, and compressive modulus of the PCL/HA, PCL-PHB/HA and PCL-PHBV/HA dual-leached scaffolds: a,b,c,d, e , f are significantly different at $p < 0.05$ for an individual feature; *one way ANOVA with Tukey HSD, and n = 10 for porosity pore volume. n = 30 for pore size

Scaffolds	Actual HA (%)	Density* (g/cm^3)	Porosity* (%)	Pore volume* (cm^3/g)	Pore size (µm)	Compressive modulus (kPa)
PCL/HA	29.29	0.3276±0.0396	71.39±3.46	2.2202±0.3820	441±23	258±24.1
PCL-10% PHB/HA	26.36	0.2263±0.0669	80.23±5.85	3.9890±1.7719	372±23	1778±7.8
PCL-20% PHB/HA	31.46	0.2135±0.0446	81.36±3.89	4.0337±1.2328	374±30	1745±6.1
PCL-30% PHB/HA	26.20	0.2119±0.0359	81.50±3.13	3.9755±0.7257	379±21	1,923±9.5
PCL-10% PHBV/ HA	36.22	0.2614±0.0383	77.17±3.34	3.0355±0.6380	367±28	2,283±7.7
PCL-20% PHBV/ HA	36.96	0.2391±0.0319	79.11±2.72	3.3703±0.5336	389±34	1,712±17.6
PCL-30% PHBV/ HA	36.07	0.2077±0.0300	81.86±2.62	4.0344±0.7278	379±27	2,866±29.6

Remaining weight after degradation

Figure 6.2 shows the remaining weight of the scaffolds after degrading in the absence and presence of the enzyme lipase in 0.1 M PBS pH 7.4 at 37°C for 13 weeks. In the absence of lipase (figure 6.2 (a)), the remaining weight of PCL/HA gradually decreased in 13 weeks and the remaining weight decreased from ~100% to ~94% in 13 weeks. The PCL/HA scaffolds showed the slightly change of remaining weight while the PCL-10%PHBV/HA, PCL-10%PHB/HA, and PCL-20%PHB/HA dual leached scaffolds did not show the rapidly change of remaining weight until the end of 13 weeks. Whereas the remaining weight of PCL-30%PHB/HA, PCL-20%PHBV/HA, and PCL-30%PHBV/HA scaffolds were rapidly significant drop and remaining weights were only 54.2%, 60.7%, and 64.8%, respectively. It can be said that the PCL-30%PHB/HA, PCL-20%PHBV/HA, and PCL-30%PHBV/HA scaffolds also showed high water uptake which is another factor in the hydrolytic degradation due to water could lead to swelling of the polymer and thus facilitate degradation. The biodegradability of these dual leached scaffolds in the absence lipase solution can be rank as follows: PCL-30%PHB/HA > PCL-20%PHBV/HA > PCL-30%PHBV/HA > PCL-20%PHBV/HA > PCL-10%PHBV/HA > PCL-10%PHB/HA > PCL/HA. In the presence of lipase (figure 6.2 (b)), it was clearly observed that the remaining weight of PCL-PHB/HA and PCL-PHBV/HA dual leached scaffolds were much decreasing compare to the absence of lipase condition except for PCL-10%PHBV/HA scaffold. For PCL/HA, PCL-10%PHB/HA, PCL-20%PHB/HA, PCL-30%PHB/HA, PCL-10%PHBV/HA, PCL20%PHBV/HA, and PCL-30%PHBV/HA dual leached scaffolds, the percentage of decreasing weight were 93.0%, 48.4%, 48.2%, 40.1%, 65.6%, 41.2%, and 41.8%, respectively. The activity of this enzyme lipase exhibited an effect to PCL-PHB/HA, and PCL-PHBV/HA dual leached scaffolds. Additionally, the degradation profiles of PCL/HA and PCL-10%PHBV/HA dual leached scaffolds were similar; they revealed the slightly decreasing of weight in 13 weeks. Whereas the degradation rate of PCL-10%PHBV/HA and PCL-10%PHBV/HA dual leached scaffolds tented to decrease rapidly on the weeks 5 and have the same range of degradation rate and the degradation rate of PCL-20%PHBV/HA, PCL-30%PHB/HA, and PCL-30%PHBV/HA dual leached scaffolds tended to decrease rapidly and dramatically

drop of weight after 5 weeks. The biodegradability of these polyester scaffolds in lipase solution can be rank as follows: PCL-30%PHB/HA > PCL-20%PHBV/HA > PCL-30%PHBV/HA >PCL-20% PHB/HA > PCL-10%PHB/HA > PCL-10%PHB/HA > PCL/HA.
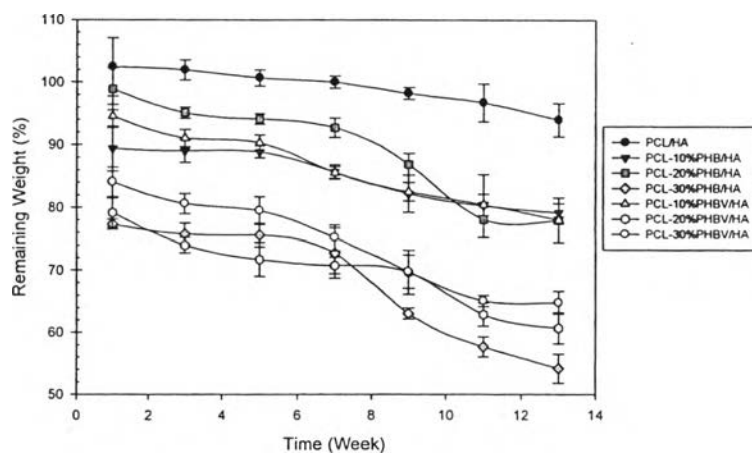
(a)
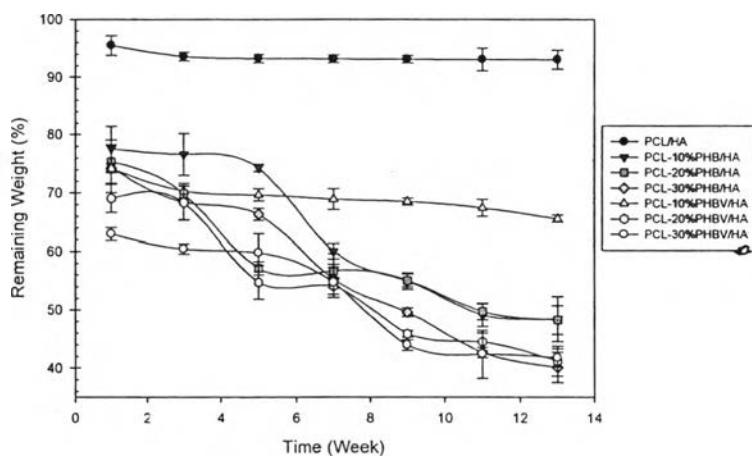
(b)

Figure 6.2 Remaining weight of the scaffolds after 13 weeks degradation in 0.1 M PBS containing (a) without lipase, (b) with lipase.

6.4.2 Biological Evaluation of PCL-PHB/HA and PCL-PHBV/HA Scaffolds

Indirect Cytotoxicity Evaluation

An Indirect cytotoxicity evaluation was conducted on TCPS, PCL/HA, PCL-PHB/HA, and PCL-PHBV/HA dual-leached scaffolds by using mouse calvaria-derived preosteoblastic cells(MC3T3-E1) and mouse fibroblasts cells (L929). Even though we were interested in using the obtained scaffolds as potential bone scaffolds, it was mandatory to test the materials with L929 just to comply with the ISO10993-5 standard test method. For both types of cells, about 40,000 cells/well were seeded in empty wells of TCPS. Figure 6.3 (a) and 6.3 (b) show the viability of the cells obtained from MTT assay after the cells had been cultured with the 1, 3, 7 day- extraction media from scaffolds as compared with that obtained after the cells had been cultured with the fresh SFM(control TCPS). The viability of the cells was reported as the percentage with respect to that of the TCPS. Evidently, the viability ratio of cells that had been cultured with all of extraction media from PCL/HA, PCL-PHB/HA, and PCL-PHBV/HA dual-leached scaffolds (and with control TCPS) were greater than 80%. These results could be suggested that all types of PCL-PHB/HA and PCL-PHBV/HA dual-leached scaffolds posed no threats to the cells.
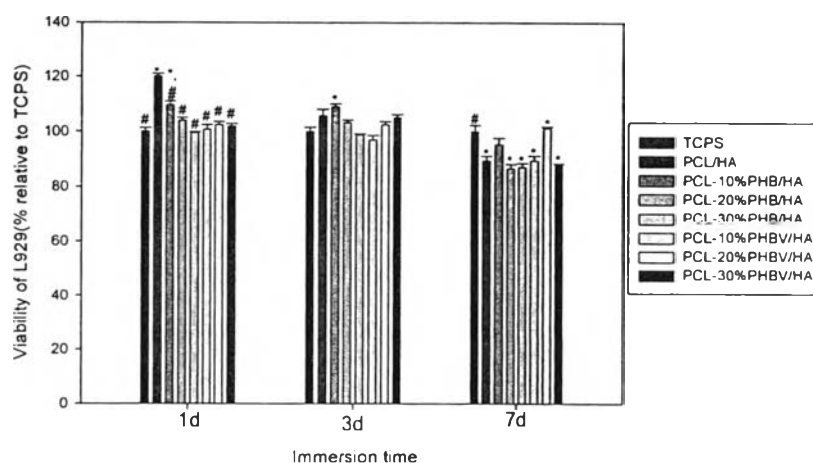
(a)
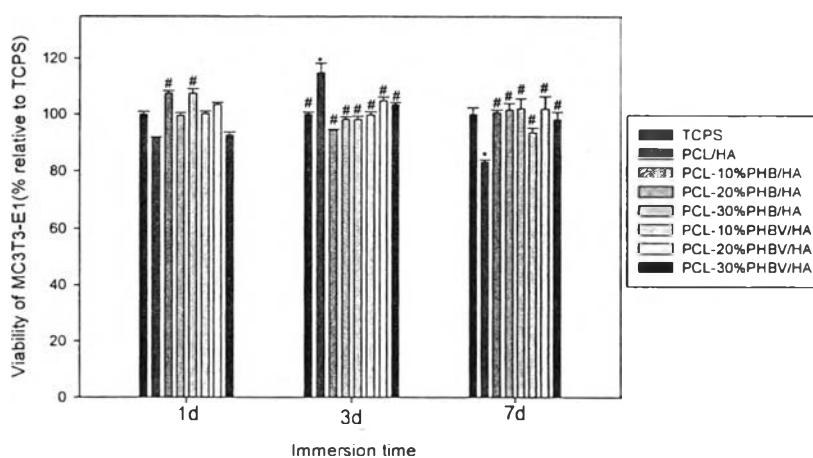
(b)

Figure 6.3 Indirect cytotoxic evaluation of TCPS, PCL/HA, PCL-10%PHB/HA, PCL-20%PHB/HA, PCL-30%PHB/HA, PCL-10%PHBV/HA, PCL-20%PHBV/HA and PCL-30%PHBV/HA dual-leached scaffolds, based on the viability of (a) mouse fibroblasts (L929) and (b) pre-osteoblasts (MC3T3-E1) that were cultured with the extraction medium from each scaffold. Cell viability was tested using cells that had been cultured with their respective culture media each day as a function of the incubation time of the extraction and the culture media of 1, 3, or 7 days. Statistical significance: $*p < 0.05$ compared with control and $^\#p < 0.05$ compared to the PCL/HA scaffolds at any given time point.

Cell Attachment and Cell Proliferation

The potential for the PCL-PHB/HA and PCL-PHBV/HA dual-leached scaffolds in supporting both the attachment and the proliferation of bone cells were assessed with MC3T3-E1. The cells were either seeded or cultured on the surfaces of the PCL/HA, PCL-PHB/HA, and PCL-PHBV/HA dual-leached scaffolds and TCPS (control) for 4, 8 16 h and 1, 2, 3 day. Figure 6.4 shows the attachment of MC3T3-E1 on the surface of TCPS, the PCL/HA, PCL-PHB/HA, and PCL-PHBV/HA dual-leached scaffolds on 4, 8, and 16 h after cell culturing in terms of the viability of cells (%relative to TCPS at 4 h). The viability of cells on a scaffold could be quantified by Fluorescent emission intensity from the Alarmar Blue assay. On TCPS, the number of cells increased from ~100% on 4 h after cell culture to ~133% on 16 h after cell culturing, based on the initial 40,000 cells/well of cells seeded. In comparison with the viability of cells on TCPS and PCL/HA, the viability of cells on PCL-PHB/HA, and PCL-PHBV/HA dual-leached scaffolds were significantly higher at any given time point. The viability of cells on PCL/HA was lower than that on TCPS at any given time point. The viability of cells on PCL-PHB/HA dual-leached scaffold was slightly lower than that on PCL-PHBV/HA on 4 h and was similar to the viability of cells on PCL-PHBV/HA on 8, and 16 h. On PCL-PHB/HA, PCL-PHBV/HA dual-leached scaffold, the viability of cells on 4, 8, and 16 h increased about ~200-250% when compared to that on TCPS.

Figure 6.5 shows the proliferation of MC3T3-E1 on the surface of TCPS, the PCL/HA, PCL-PHB/HA, and PCL-PHBV/HA dual-leached scaffolds on day 1, 2, and 3 after cell culturing in terms of the viability of cells (%relative to TCPS at day1). The viability of cells on a scaffold could be quantified by Fluorescent emission intensity from the Alarmar Blue assay. On TCPS, the number of cells increased from ~100% on day1 after cell culture to ~147% on day 3 after cell culturing, based on the initial 40,000 cells/well of cells seeded. In comparison with the viability of cells on TCPS, the viability of cells on all PCL/HA, PCL-PHB/HA, and PCL-PHBV/HA dual-leached scaffolds were significantly higher at any given time point. The viability of cell on the PCL-PHB/HA and PCL-PHBV/HA dual-leached scaffolds were higher than that on PCL/HA dual-leached scaffold on day 1 and were significantly higher than that on PCL/HA dual-leached scaffold on day 2

and 3. The viability of cell on the PCL-PHB and PCL-PHBV dual-leached scaffolds were not different on day 1. The viability of cell on the PCL-PHB/HA dual-leached scaffolds were greater than that on PCL-PHBV/HA dual-leached scaffold at any given time point and the viability of cell on the PCL-20%PHB/HA, and PCL-30%PHB/HA scaffolds shows the highest on day 3. For the proliferation of the cells, all PCL-PHB/HA and PCL-PBV/HA dual-leached scaffolds are able to support the proliferation of the cells at significantly higher levels to that on TCPS, this results could be suggested that the PCL-PHB/HA and PCL-PHBV/HA dual-leached scaffolds provided better support for bone cell adhesion and proliferation.
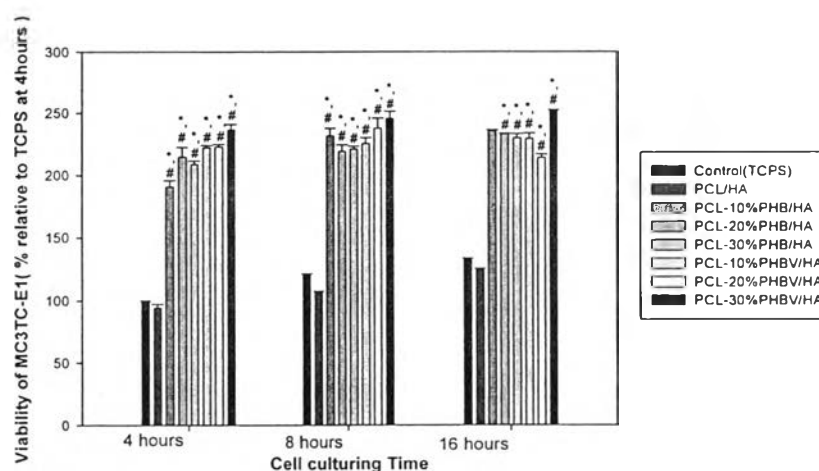
Figure 6.4 Attachment of MC3T3-E1 cells that were seeded or cultured on the surfaces of TCPS, PCL/HA, PCL-10%PHB/HA, PCL-20%PHB/HA, PCL-30%PHB/HA, PCL-10%PHBV/HA, PCL-20%PHBV/HA and PCL-30%PHBV/HA dual-leached scaffolds for 4, 8, or 16 hours. Statistical significance: $*p < 0.05$ compared with control and $^{\#}p < 0.05$ compared to the PCL/HA scaffolds at any given time.
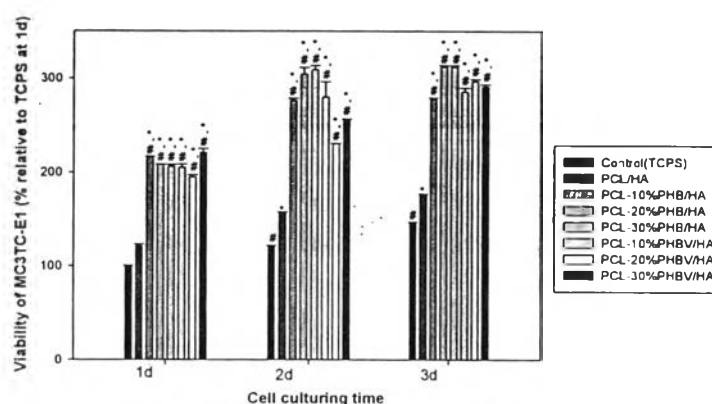
Figure 6.5 Proliferation of MC3T3-E1 cells that were seeded or cultured on the surfaces of TCPS, PCL/HA, PCL-10%PHB/HA, PCL-20%PHB/HA, PCL-30%PHB/HA, PCL-10%PHBV/HA, PCL-20%PHBV/HA and PCL-30%PHBV/HA dual-leached scaffolds for 1, 2, or 3 days. Statistical significance: $*p < 0.05$ compared with control and $^{\#}p < 0.05$ compared to the PCL/HA scaffolds at any given time.

Cell Morphology

Table 6.3 and 6.4 show selected SEM images (magnification = 3500X; scale bar = 5 μm) of MC3T3-E1 that were either seeded or cultured on the surfaces of glass, PCL-PHB/HA, and PCL-PHBV/HA dual-leached scaffolds at different time points. According to these images, cell morphology and interaction between cells and the scaffolds can be investigated. At 4 h after cells seeding, the majority of cells on the glass surface was stilled rounded and started to extend their cytoplasm. At 8 h after cells seeding, the majority of cells on the glass surface showed evidence of the extension of their cytoplasm on the surface. At 16 h after cells seeding, the majority of cells showed evidence of the expansion on the surface. For the cells that were seeded on the surface of all scaffolds, at 4 h after cells seeding, the majority of cells on surface showed evidence of the extension of their cytoplasm on the surface. At 8 h after cells seeding, the majority of cells showed evidence of the extension and expansion on the surface. At 16 h after cells seeding, the majority of cells expanded over the area of scaffolds which were the most

expansion on PCL-10%PHB/HA, PCL-20%PHB/HA, PCL-20%PHBV/HA, and PCL-30%PHBV/HA dual-leached scaffolds. At 1, 2, and 3 days after cells seeding, the majority of the cells seeded on the surfaces of all types of scaffolds expanded over the area of the scaffolds. The most expansion were on the surface of PCL-20%PHB/HA dual-leached scaffold at any given time point.

Table 6.3 Attachment of MC3T3-E1 that had been seeded or cultured on the surfaces of glass, the PCL-PHB/HA and the PCL-PHBV/HA dual-leached scaffolds for 4, 8, or 16 h. Selected SEM images of cultured specimens, i.e., glass (i.e., control), PCL-PHB/HA, and PCL-PHBV/HA dual-leached scaffolds at three different time points after MC3T3-E1 were seeded or cultured on their surfaces (magnification = 3500X; scale bar = 5 μm)
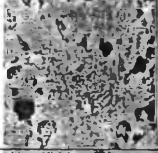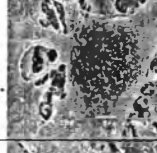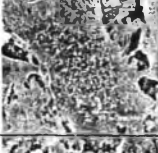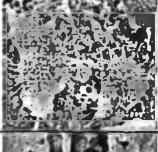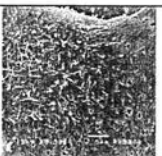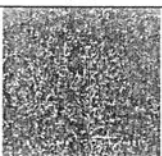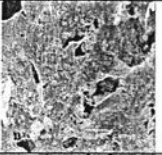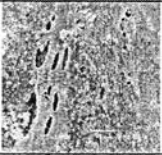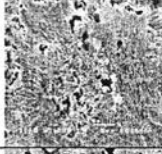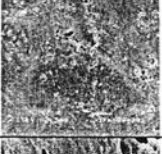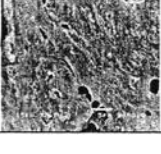
Culturing time		4h	8h	16h
Substrate	Glass			
	PCL-10% PHB/HA			
	PCL-20% PHB/HA			
	PCL-30% PHB/HA			
	PCL-10% PHBV/HA			
	PCL-20% PHBV/HA			
	PCL-30% PHBV/HA			

Table 6.4 Proliferation of MC3T3-E1 that had been seeded or cultured on the surfaces of TCPS, the PCL-PHB/HA, and the PCL-PHBV/HA dual-leached scaffolds for 1, 2, or 3d. Selected SEM images of cultured specimens, i.e., glass (i.e., control), PCL/HA, PCL-PHB/HA, and PCL-PHBV/HA dual-leached scaffolds at three different time points after MC3T3-E1 were seeded or cultured on their surfaces (magnification = 3500X; scale bar = 5 μm)

Culturing time		1d	2d	3d
Substrate	Glass			
	PCL-10%PHB/HA			
	PCL-20%PHB/HA			
	PCL-30%PHB/HA			
	PCL-10%PHBV/HA			
	PCL-20%PHBV/HA			
	PCL-30%PHBV/HA			

Alkaline Phosphatase (ALP) Activity

Among the various biological functions of osteoblasts, secretion of alkaline phosphatase (ALP) is an important indicator determining the activity of the cells on a scaffold. The ALP activity of MC3T3-E1 on TCPS (i.e. controls), PCL/HA, PCL-PHB/HA, and PCL-PHBV/HA dual-leached scaffolds were monitored at 3, 5 and 7 days in culture (see Figure 6.6). For all of PCL/HA, PCL-PHB/HA and PCL-PHBV/HA scaffolds investigated, the ALP activities were lower than TCPS on day 3, 5, and 7 except for PCL-30%PHBV/HA on day 3. The ALP activities of PCL-20%PHBV/HA and PCL-30%PHBV/HA were higher than PCL/HA on day 3. The ALP activities of PCL-PHBV/HA were higher than PCL-PHB/HA on day 3. The ALP activities of PCL-PHB/HA and PCL-PHBV/HA were similar to ALP activities of PCL/HA on day 5. The ALP activities of PCL-PHBV/HA were higher than ALP activities of PCL-PHB/HA on day 7. Since ALP activity is also detected in several non-calcified tissues and organs as the kidney, small intestines and placenta, it could be indicated that the ALP acitivity of MC3T3-E1 that were cultured on scaffolds could not be a marker of the calcification process.[43-46]
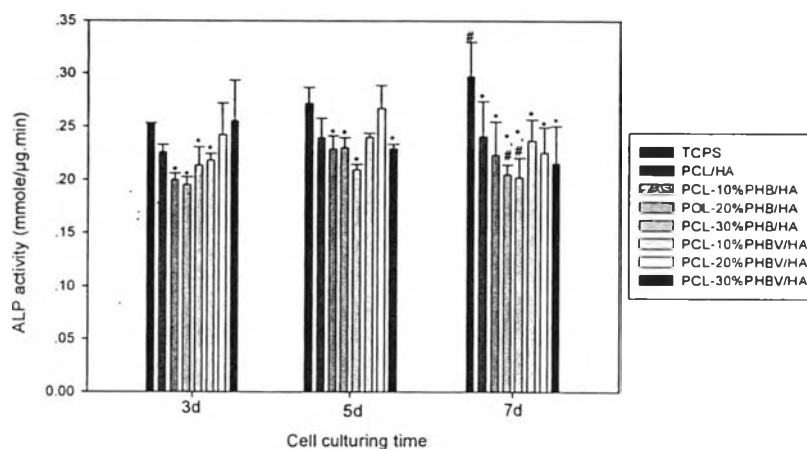
Figure 6.6 Alkaline phosphatase (ALP) activity of MC3T3-E1 cells that were cultured on the surfaces of TCPS, PCL/HA, PCL-10%PHB/HA, PCL-20%PHB/HA, PCL-30%PHB/HA, PCL-10%PHBV/HA, PCL-20%PHBV/HA and PCL-30%PHBV/HA dual-leached scaffolds for 3, 5, or 7 days. Statistical significance: *p < 0.05 compared with control and #p < 0.05 compared to the PCL/HA scaffolds at any given time.

Mineralization

Alizarin Red S staining was used to quantify the mineral deposition of MC3T3-E1 that were cultured on the surfaces of TCPS, PCL/HA, PCL-PHB/HA, and PCL-PHBV/HA dual-leached scaffolds for 14 and 21 days. Table 6.5 shows photographic images of the stained specimens. The appearance of red on the stained product shows the presence of calcium. In the presence of calcium, the Alizarin Red S-calcium chelating product appeared red. On day 14 after cell culturing, the red staining product observed for PCL-20%PHB/HA dual-leached scaffolds was greatest, followed by that observed for PCL-10%PHB/HA, and PCL-10%PHBV/HA. An increase in the red staining product was observed for all the surfaces investigated on day 21. The quantitative analysis of the results shown in Figure 6.7 was carried out by elution of calcium deposition with cetylpyridinium chloride and spectrophotometically read at 570 nm. The extracted stain absorbance obtained on days 14 supported the above data where highest intensity of staining product was

observed on PCL-PHB/HA, followed by PCL-PHBV/HA, PCL/HA, and TCPS respectively. When the culture was maintained up to 21 days, significantly greater amount of calcium deposition were observed on PCL-20%PHB/HA scaffolds.
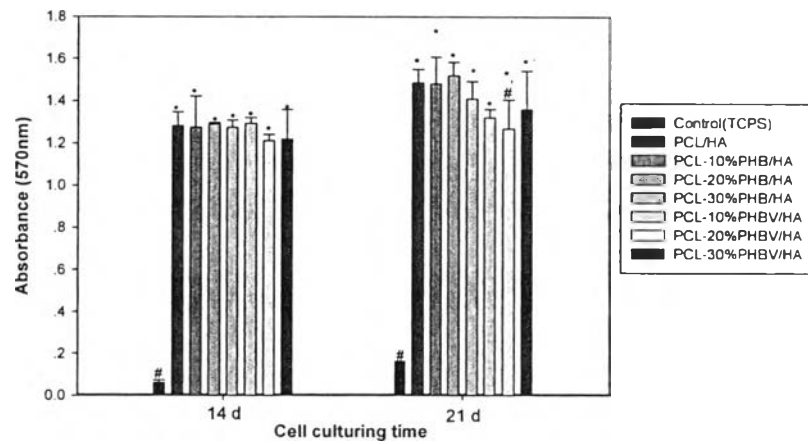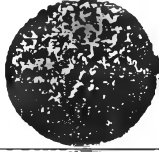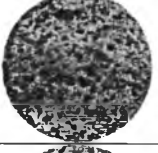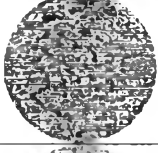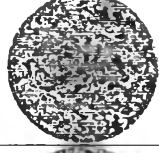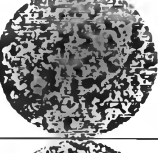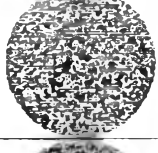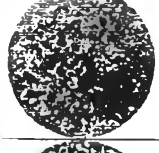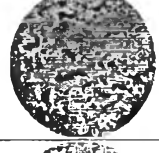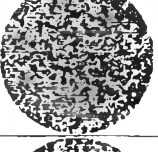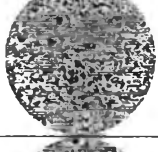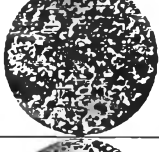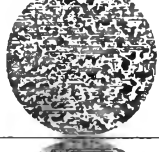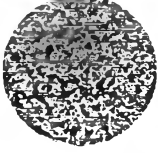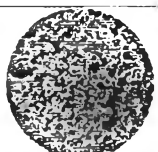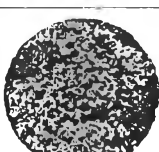
Figure 6.7 Quantification of mineral deposition in MC3T3-E1 cells by Alizarin Red-S staining. Statistical significance: $*p < 0.05$ compared with control and $^{\#}p < 0.05$ compared to the PCL/HA scaffolds at any given time point.

Table 6.5 Images of Alizarin Red-S staining for the mineralization in MC3T3-E1 on the TCPS, the PCL/HA, the PCL-PHB/HA, and the PCL-PHBV/HA dual-leached scaffolds at 14 and 21 day

Substrate	Day			
	14 Day		21 Day	
	+ Cell	- Cell	+ Cell	-Cell
TCPS				
PCL/HA				
PCL-10% PHB/HA				
PCL-20% PHB/HA				
PCL-30% PHB/HA				
PCL-10% PHBV/HA				
PCL-20% PHBV/HA				
PCL-30% PHBV/HA				

6.5 Conclusion

In this study, PCL-PHB/HA and PCL-PHBV/HA dual-leached scaffolds have been prepared by using solvent casting and salt particulate leaching with polymer leaching technique. Scanning electron microscopy (SEM) images confirmed that these scaffolds were characterized by highly interconnected networks, porosity, and a pore size of 367-389 μm. The mechanical properties, porosities, pore volumes, water absorption capacities, and weight remaining after degradation were also investigated. An indirect cytotoxicity evaluation with mouse fibroblastic cells (L929) and mouse calvaria-derived pre-osteoblastic cell (MC3T3-E1) revealed that the scaffolds fabricated using our method released no substances at levels that were harmful to the cells. The potential for the use of these constructs in bone tissue engineering was evaluated in vitro using mouse calvaria-derived pre-osteoblastic cells (MC3T3-E1) that were seeded or cultured at different time. For the attachment and proliferation of the cells, all PCL-PHB/HA and PCL-PHBV/HA dual-leached scaffolds are able to support the proliferation of the cells at significantly higher levels to that on TCPS and PCL/HA, this results could be suggested that the PCL-PHB/HA and PCL-PHBV/HA dual-leached scaffolds provided better support for bone cell adhesion and proliferation. For the cells that were seeded on the surface of all scaffolds, the majority of cells appeared to be well-expanded and attach on scaffolds surface while that seeded on glass substrate was still in round shape on 4 h. At 1, 2, and 3 days after cells seeding, the majority of the cells seeded on the surfaces of all types of scaffolds expanded over the area of the scaffolds. In mineralization assessment of MC3T3-E1 on days 14 and 21, the most intensity of staining product for calcium deposition was observed on PCL-20%PHB/HA scaffold. Our results indicate that PCL-PHB/HA and PCL-PHBV/HA dual-leached scaffold possess its ability to support MC3T3-E1 cell attachment, proliferation, and mineralization for used as bone scaffolding material.

6.6 Acknowledgements

6.7 References

[1]   Masami, O. and Baiju J. (2013) Synthetic biopolymer nanocomposites for tissue engineering scaffolds. Progress in Polymer Science, 38, 1487– 1503

[2]   Wang ,Y., Liu, L., and Guo, S. (2010) Characterization of biodegradable and cytocompatible   nano-hydroxyapatite/polycaprolactone   porous   scaffolds   in degradation in vitro. Polymer Degradation Stability, 95, 207-213

[3]   Rezwana, K., Chena, Q.Z., Blakera, J.J., and Aldo, R.B.   (2006) Biodegradable and bioactive porous polymer/inorganic composite scaffolds for bone tissue engineering. Biomaterials, 27, 3413–3431

[4]   Yung-Chih, K., and Cheng-Ting, W. (2012) Neuronal differentiation of induced pluripotent stem cells in hybrid polyester scaffolds with heparinized surface. Colloids and Surfaces B: Biointerfaces, 100, 9– 15

[5]   Kai, Z., Ying, D., Jin, C.C., and Guo-Qiang, C. (2003) Polyhydroxyalkanoate (PHA) scaffolds with good mechanical properties and biocompatibility. Biomaterials, 24, 1041–1045

[6]   Ilaria, C., Manuela, C., and Alessandra, B. (2013) Tailoring the properties of electrospun PHBV mats: Co-solution blending and selective removal of PEO. European Polymer Journal, 49, 3210–3222

[7]   Long, Y., Katherine, D., and Lin, L. (2006) Polymer blends and composites from renewable resources. Progress in Polymer Science, 31, 576–602

[8]   Perrine, B., Eric, P., and Luc, A. (2009) Nano-biocomposites: Biodegradable polyester/nanoclay systems. Progress in Polymer Science, 34, 125–155

[9]   Murali, M.S., Singaravelu, V., Manjusri, M., Sujata, K. B., and Amar, K. M. (2013) Biobased plastics and bionanocomposites: Current status and future opportunities. Progress in Polymer Science, 38, 1653– 1689

[10]   Hutmacher, D.W. (2001) Scaffold design and fabrication technologies for engineering tissues--state of the art and future perspectives. Biomaterial Science Polymer Edition, 12 (1), 107-241

[11]   Lida, B. H., Yashchuk, O., and Miyazaki, S.S. (2009) Changes in the mechanical properties of compression moulded samples of poly(3-hydroxybutyrate-co-3-hydroxyvalerate) degraded by Streptomyces omiyaensis SSM 5670E´. Polymer Degradation and Stability, 94, 267–271

[12]   Jian, T., Cunjiang, S., Mingfeng, C., Dan, H., Li, L., Na, L., and Shufang, W. (2009) Thermal properties and degradability of poly(propylene carbonate)/poly(b-hydroxybutyrate-co-b-hydroxyvalerate) (PPC/PHBV) blends. Polymer Degradation and Stability, 94, 575–583

[13]   Marrakchi, Z., Oueslati, H., Belgacem, M.N., Mhenni, F., and Mauret, E. (2012) Biocomposites based on polycaprolactone reinforced with alfa fibre mats. Composites: Part A, 43, 742–747

[14]   Lijun, J., Wenjun, W., Duo, J., Songtao, Z., and Xiaoli, S. (2015) In vitro bioactivity and mechanical properties of bioactive glass nanoparticles/polycaprolactone composites. Materials Science and Engineering C, 46, 1–9

[15]   Carletti, E., Motta, A., and Migliaresi, C.(2011) Scaffolds for Tissue Engineering and 3D Cell Culture. Methods Molecular Biology, 695, 17-39

[16]   Xian-Yi, X., Xiao-Tao, L., Si-Wu, P., Jian-Feng, X., Chao, L., Guo, F., Kevin, C. C., and Guo-Qiang, C. (2010) The behaviour of neural stem cells on polyhydroxyalkanoate nanofiber scaffolds. Biomaterials, 31, 3967–3975

[17]   Donghua, G., Zhiqing, C., Chunpeng, H., and Yinghe, L. (2008) Attachment, proliferation and differentiation of BMSCs on gas-jet/electrospun nHAP/PHB fibrous scaffolds. Applied Surface Science, 255, 324–327

[18]   Shuai, W., Piming, M., Ruyin, W., Shifeng, W., Yong, Z., and Yinxi, Z. (2008) Mechanical, thermal and degradation properties of poly(d,l-lactide)/poly(hydroxybutyrate-co-hydroxyvalerate) /poly(ethylene glycol) blend. Polymer Degradation and Stability, 93, 1364–1369

[19]   Amir, N. H., Hosseinalipour, S.M., Rezaie, H.R., and Shokrgozar, M.A. (2012) Characterization of poly(3-hydroxybutyrate)/nano-hydroxyapatite composite scaffolds fabricated without the use of organic solvents for bone tissue engineering applications. Materials Science and Engineering C, 32, 416–422

[20]   Shaun, E. and Suman, D. (2010) Mechanical and microstructural properties of polycaprolactone scaffolds with one-dimensional, two-dimensional, and three-dimensional orthogonally oriented porous architectures produced by selective laser sintering. Acta Biomaterialia, 6, 2467–2476

[21]   MyllymaÈ, K.O., MyllaÈ, R.P., Forssell, P., Suortti, T., LaÈ hteenkorva, K., Ahvenainen, R., and Poutanen, K. (1998) Mechanical and Permeability Properties of Biodegradable Extruded Starch/polycaprolactone Films. PACKAGING TECHNOLOGY AND SCIENCE, 11, 265-274

[22]   Ken-Jer, W., Chin-San, W., and Jo-Shu, C. (2007) Biodegradability and mechanical properties of polycaprolactone composites encapsulating phosphate-solubilizing bacterium Bacillus sp. PG01. Process Biochemistry, 42, 669–675

[23]   Chern, C. E., Nor, A. I., Norhazlin, Z., Hidayah, A.,Wan, Md., Zin, W. Y., Yoon, Y. T., and Cher, C. T. (2013) Enhancement of Mechanical and Thermal Properties of Polylactic Acid/Polycaprolactone Blends by Hydrophilic Nanoclay. Indian Journal of Materials Science, 11

[24]   Jian-Zhong, H., Yong-Chun, Z., Li-Hua, H., and Hong-Bin, L. (2013) Development of biodegradable polycaprolactone film as an internal fixation material to enhance tendon repair: an in vitro study. BMC Musculoskeletal Disorders, 14, 246

[25]   Sanaz, A., Samira, S., Nor Azowa, I., Wan, M. Z., Wan, Y., Mohamad, Z. A. R., Susan, A., and Asma, F. (2012) Enhancement of Mechanical and Thermal Properties of Polycaprolactone/Chitosan Blend by Calcium Carbonate Nanoparticles.

International Journal of Molecular Science, 13, 4508-4522

[26]   Azadeh, A., Mohammad, T. K., Aliasghar, B., Babak, F., and Shahin, B. (2011) Manufacturing of biodegradable polyurethane scaffolds based on polycaprolactone using a phase separation method: physical properties and in vitro assay. International Journal of Nanomedicine, 6, 2375–2384

[27]   Steaphane, S.and Monique, L. (2006) Physicochemical Properties of Alginate/ Polycaprolactone-Based Films Containing Essential Oils. Journal of Agriculture Food Chemistry, 54, 10205-10214

[28]   Thadavirul, N., Pavasant, P., and Supaphol, P. Fabrication and evaluation of polycaprolactone-poly(hydroxybutyrate)   or   poly(3-hydroxybutyrate-co-3-hydroxyvalerate) dual-leached porous scaffolds for bone tissue engineering applications, in preparation.

[29]   Chunyan, Z., Aaron, T., Giorgia, P., and Han, K. H. (2013) Nanomaterial scaffolds for stem cell proliferation and differentiation in tissue engineering. Biotechnology Advances, 31, 654–668

[30]   Christina, W. C., Loran, D. S., and Eben, A. (2014) Decellularized tissue and cell-derived extracellular matrices as scaffolds for orthopaedic tissue engineering. Biotechnology Advances , 32, 462–484

[31]   Chuenjitbuntaworn, B., Supaphol, P., Pavasant, P., and Damrongsri, D. (2010) Electrospun poly(L-lactic acid)/hydroxyapatite composite fibrous scaffolds for bone tissue engineering. Polymer International, 59, 227-235

[32]   Wutticharoenmongkol, P., Sanchavanakit, N., Pavasant, P.,and Supaphol, P. (2006) Novel Bone Scaffolds of Electrospun Polycaprolactone Fibers Filled withNanoparticles. Journal of Nanoscience Nanotechnology, 6, 514-522

[33]   Cai, L., Guinn, A.S., and Wang, S. (2011) Exposed hydroxyapatite particles on the surface of photo-crosslinked nanocomposites for promoting MC3T3 cell proliferation and differentiation. Acta Biomaterialia, 7, 2185-2199

[34]   Choi, J.Y., Lee, B.H., Song, K.B., Park, R.W., Kim, I.S., Sohn, K.Y., Jo, J.S., and   Ryoo, H.M. (1996) Expression Patterns of Bone-Related Proteins During Osteoblastic Differentiation in MC3T3-El Cells. Journal of Cell Biochemistry, 61(4), 609-618.

[35] Yu, H.S., Hong, S.J., and Kim, H.W. (2009) Surface-mineralized polymeric nanofiber for the population and osteogenic stimulation of rat bone-marrow stromal cells. Material Chemistry Physic, 113, 873–877.

[36] Tsukamoto, Y., Fukutani, S., and Mori, M. (1992) Hydroxyapatite-induced alkaline phosphatase activity of human pulp fibroblasts. Journal of Material Science: Material Medical, 3, 180-183.

[37] Calvert, J.W., Marra, K.G., Cook, L., Kumta, P.N., DiMilla, P.A., and Weiss, L.E. (2000) Characterization of osteoblast-like behavior of cultured bone marrow stromal cells on various polymer surfaces. Journal of Biomedical Material Research, 52, 279

[38] Sun, F., Zhou, H., and Lee, J. (2011) Various preparation methods of highly porous hydroxyapatite/polymer nanoscale biocomposites for bone regeneration. Acta Biomaterialia, 7, 3813-3828

[39] Deplaine, H., Gomez, Ribelles J.L., and Gallego, F.G. (2010) Effect of the content of hydroxyapatite nanoparticles on the properties and bioactivity of poly(L-lactide) – Hybrid membranes. Composite Science Technology , 70, 1805-1821

[40] Ma P.X. (2008) Biomimetic materials for tissue engineering. Advance Drug Deliver Revision, 60, 184-198

[41] Puppi, D., Chiellini, F., Piras, A.M., and Chiellini, E. (2010) Polymeric materials for bone and cartilage repair. Polymer Science, 35, 403-440

[42] Thadavirul, N., Pavasant, P., and Supaphol, P. (2013) Development of polycaprolactone porous scaffolds by combining solvent casting, particulate leaching, and polymer leaching techniques for bone tissue engineering. Journal of Biomedical Material Research: Part A, 00A, 000-000

[43] Thadavirul, N., Pavasant, P., and Supaphol, P. (2014) Improvement of dual-leached polycaprolactone porous scaffolds by incorporating with hydroxyapatite for bone tissue regeneration. Journal of Biomaterials Science, Polymer Edition, 0,000-000

[44] Lee, S.C., Choi, H.W., Lee, J.H., Kim, K.J., Chang, J.H., Kim, S.Y., Choi, J., Oh, K.S., and Jeong, Y.K. (2007) In-situ synthesis of reactive hydroxyapatite nano-crystals for a novel approach of surface grafting polymerization. Journal of Material Chemistry, 17, 174-180

[45]   Karageorgiou, V., and Kaplan, D. (2005) Porosity of 3D biomaterial scaffolds and osteogenesis. Biomaterial, 26, 5474-5491

[46]   Joel, R., and Michel, A. H. (2006) Preparation of interconnected poly(ε-caprolactone) porous scaffolds by a combination of polymer and salt particulate leaching. Polymer, 47, 4703–4717